

Figure 32: Representation of the signal vs. time response for an APV25 module.

The advantage to using such a shaping signal, is that three samples can be used to deconvolute the longer, shaped signal to suppress out-of-time background hits. Assuming the form given in Eq. 15, the signal in time sample  $k$  is given by

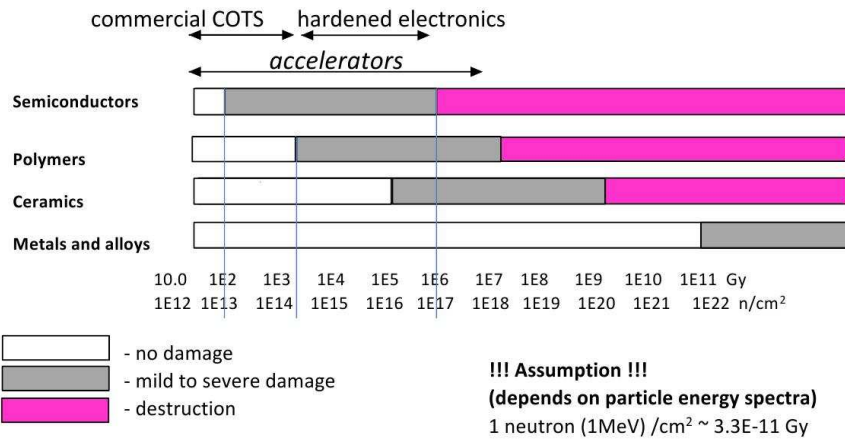
$$s_k = w_1 v_k + w_2 v_{k-1} + w_3 v_{k-2} \quad (16)$$

where weights  $w_i$  are proportional to

$$w_1 \sim e^x/x, w_2 \sim 2/x, w_3 \sim e^{-x}/x. \quad (17)$$

### 3.6 Background and Radiation damage estimates

The simulation and background calculation software for SoLID is using the two simulation packages with independent code base (Geant4 and FLUKA [13] [14]). This allows independent cross checks both in geometry and in physics modelling. At the same time the two codes each provide unique capabilities expanding the overall reach. FLUKA provides useful tools that simplify the study of radiation damage and estimates but the physics processes present in the simulation lack of direct electro-nuclear dissociation and fragmentation models. Such electro-nuclear reactions are dominant in the neutron production from the Liq.D target at high energies (see figure 38). If one just considers the neutron photo-production, both codes (GEANT4 and FLUKA) have really good agreement with experimental cross section, as shown in figure 36 and 37. A full simulation and tests are underway in order to construct a better and common target background generator for both simulation packages (see figure 38). To have a first idea of the tolerance of different



© Lockheed Martin

Figure 33: Estimate of the tolerance of different material to different level of radiation exposure given in Gy and  $\frac{\text{neutron}(1\text{MeV})}{\text{cm}^2}$ . This is just a first order approximation and a detailed analysis of each equipment is needed in order to establish the correct radiation tolerance of each detector/material

1976 material to radiation damage, see figure 33. As a weighting factor to estimate the  
 1977 effect of radiation damage on electronics I used, in parallel to the calculation of full  
 1978 Dose estimates, the Displacement damage in silicon, on-line compilation curves  
 1979 by A. Vasilescu (INPE Bucharest) and G. Lindstroem (University of Hamburg).  
 1980 This curves assume that the damage effects by energetic particles in the bulk of  
 1981 any material can be described as being proportional to the so called Non Ionising  
 1982 Energy Loss and normalise the damage in Silicon to the one caused by a 1 MeV  
 1983 neutron (more details can be found here [16]).

### 1984 3.6.1 Radiation damage to GEM electronics

1985 A simulation in order to test the radiation level on the GEM foils has been done.  
 1986 Comparison to estimated radiation level of the CMS experiment, which shares the  
 1987 part of the electronics most susceptible to radiation damage for the GEM chambers  
 1988 detectors, permitted us to establish a radiation limit flux for our expected running  
 1989 time. Already with our first conceptual design of the shielding we are able to reach  
 1990 tolerable radiation levels also in the first layer of the GEM chambers (the one that  
 1991 is supposed to sustain the higher radiation fluxes). This result is show in figure 39

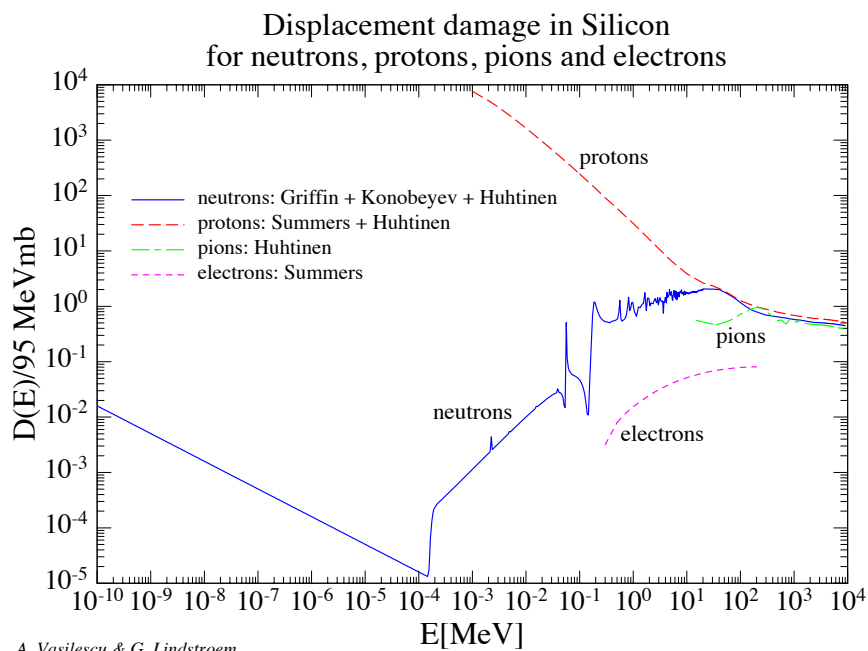


Figure 34: Not Ionising Energy Loss curves to 1MeV equivalent damage in Silicon for electrons, pions, neutrons and protons

### 1992 3.6.2 Power deposited

1993 A detailed study of the power deposited in the SoLID spectrometer has been done  
 1994 in order to detect areas of possible activation. In these areas, in order to define pos-  
 1995 sible activations, the FLUKA simulation has been used as a tool, and particle fluxes  
 1996 were provided by GEANT4 for areas where the particle fluxes estimated by  
 1997 FLUKA were known to be incorrect. FLUKA in fact provides many good tools for  
 1998 activation and radiation estimates, but lacks in direct electro-nuclear dissociation-  
 1999 fragmentation models and has limitations in producing more complex geometry,  
 2000 like the Baffle design for the PVDIS experiment in SoLID. In the following study of  
 2001 activation, GEANT4 has been used as a common input for an estimate of the back-  
 2002 ground radiation in areas where direct electro-nuclear dissociation-fragmentation  
 2003 models are important.

2004 **Power in 1st baffle (due to Mollers), (Cooling, activation)** The first baffle, due  
 2005 to his proximity to the Deuterium target in the PVDIS configuration for SoLID,

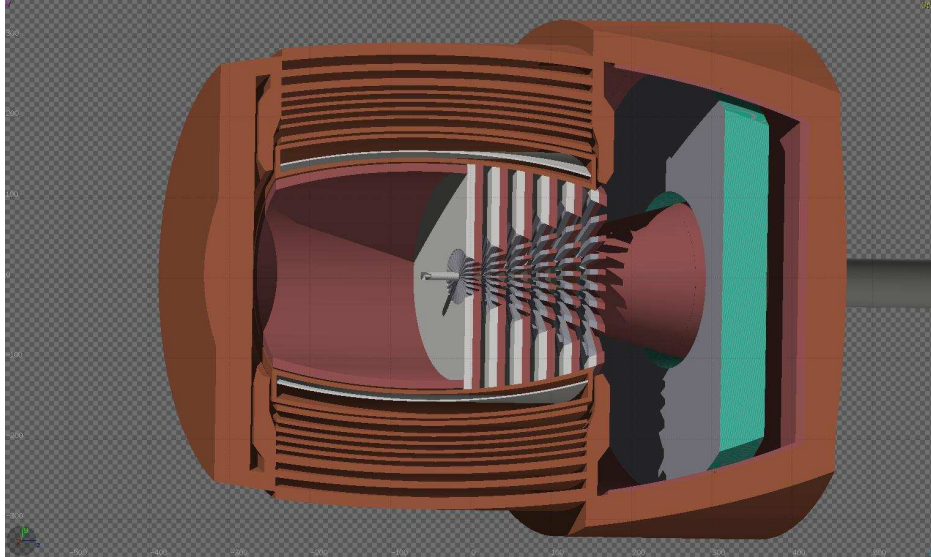


Figure 35: FLUKA simulation for the PVDIS experiment with SoLID. A first conceptual design for the neutron shielding is shown in

has a power deposition of  $\sim 8W$  for a beam current of  $50\mu A$  and an energy of  $6.6GeV$ . The high production of neutrons from the Deuterium target can be an ulterior source for activation in the baffle. For this reason an investigation of the possible activation has been done. In this study has been considered at the same time the radiation coming from the target and from the baffle itself that “self-irradiate” different parts of its structure. These results (see show the Dose equivalent radiation spatial distribution for 3 different cooling times. This study (see figure 40 ) shows, for example, that, in order to survey the area in proximity of the first baffle, one should wait around 1 day of cooling, in order to reach level of radiation tolerable. The Residual nuclei activated in the Lead baffle are shown for the same cooling time in the bottom plots of figure 40.

**Power in exit hole in magnet (elastics) (Cooling, activation)** Another spot for possible activation will be the part close to the exit hole of the magnet. Further investigation will need to be done, after a final design of the magnet will be reached, but it is expected to be less important than the activation on the first baffle, due to the not proximity to the target and to the less intense and less localise radiation. This situation has been investigated and compared to the PVDIS design, because it is the one with the expected higher activation of all the configuration with SoLID,

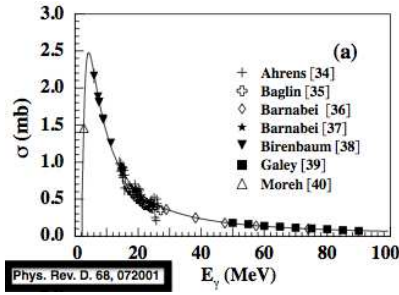


Figure 36: Neutron cross section for photo-production [15]

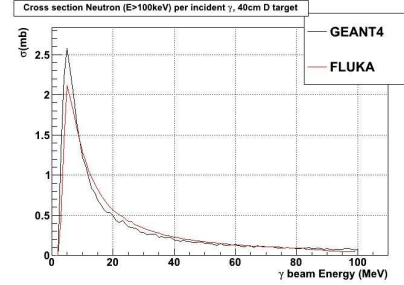


Figure 37: Test for Neutron cross section for photo-production with FLUKA and GEANT4

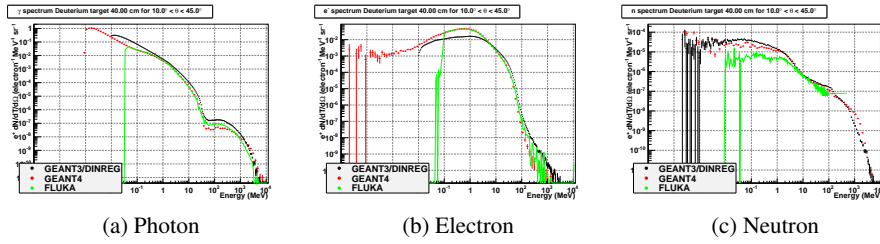


Figure 38: Background comparison produced from GEANT3(DINREG), GEANT4 and FLUKA with 40cm of Liquid Deuterium. Here is plotted the  $\frac{d^2N}{dT d\Omega}$  per incoming electron in the angle range of  $10^\circ < \theta < 45^\circ$  for  $\gamma$ (a),  $e^-$ (b) and  $n$ (c)

with the proximity of the lead baffles to the target (see this section at page 67). This has been done in order to compare power deposition to have a first idea of possible activation areas. The levels of power deposited in the exit hole of the magnet are at least lower by one order of magnitude respect to the expected in the first baffle, as shown in figure 42a and 42b. The integrated value (using the cylindrical symmetry) over the higher area of power deposition in the exit hole of the magnet has a maximum of  $\sim 0.9W$  per cm in the  $z$  direction over the full internal section of the exit hole with  $r_{xy} < 40cm$  (colour scale of  $\sim 3E-04$  in figure 42a ). This compares to a full power deposition on the first baffle of  $\sim 20W$ , running in the same conditions. A power deposition estimate for the beam-line downstream is shown in figure 42b. As one can see in 43c, is considerably smaller the impact of the configurations like SIDIS to the activation in this area.

2036 **Power in the entrance surface of the magnet (Cooling, activation) (external**  
2037 **target configurations)** With configuration like SIDIS that have the target posi-  
2038 tioned outside the magnet, there is a consistent power deposition in the front part  
2039 of the magnet. Some simulation has been done in order to estimate the possible  
2040 activation in this area. The results of these studies are presented in figure 43 and  
2041 show the areas of power deposition in the magnet and in the front surface of the  
2042 magnet. As expected the areas of possible activation is the area more exposed to  
2043 the target radiation and the collimator positioned in front of the nosecone of the  
2044 magnet.

2045 **Heat load in magnet cryostat** The power deposited from Neutron radiation on  
2046 magnet cryostat has been studied and it is expected to be less than 1W. The energy  
2047 distribution of the Neutrons irradiating the magnet cryostat is shown in figure 41.

### 2048 **3.6.3 Estimates for radiation damage in the Hall**

2049 A study has been done in order to address possible radiation damage areas with the  
2050 current SoLID design with no further shielding in place. This work has been done  
2051 in order to address and pinpoint areas that will need to be further investigated when  
2052 a final design for the magnet and electronics will be reached.

2053 **Radiation damage to electronics in Hall** The results of the different simulations  
2054 run suggest that the design of a shielding structure to minimise the radiation in the  
2055 Hall seems not to be a priority. With the current different layouts of the multiple  
2056 configuration possible with the SoLID spectrometer. In this study the magnet has  
2057 been placed in a dome structure of concrete that mimics the presence of the Hall (It  
2058 is important to consider that the SoLID spectrometer will not be placed in an open  
2059 environment, but in an Hall full of equipments, with relative reflectivity that could  
2060 cause an enhancement of the radiation present in the Hall). Different features of  
2061 these results are in common with the different configurations for SoLID:

- 2062 • The radiation damage estimated with the simulation is, as expected, consis-  
2063 tently lower in the area outside the SoLID spectrometer respect to the one  
2064 inside the magnet.
- 2065 • In the downstream part of the Hall, the predominant part of the radiation that  
2066 escape the magnet is present in the last part of the beam-line, enhancing the  
2067 choice of keeping in the upstream section of the Hall the existing left and  
2068 right arm spectrometers existing in Hall-A.

- The configurations that have the target area external to the solenoid have also an high radiation area in the proximity of the target

The configuration that gives the higher radiation estimates in this simulation study, is the PVDIS configuration with Deuterium target. The radiation damage estimate in this configuration is investigated in detail in the next section.

**Radiation from beam pipe** The main source of radiation leaking from the magnet to the Hall is from the beam pipe downstream. In order to quantify the leaking with the different layouts with SoLID, different simulation have been carried out. The one that presents the biggest impact on possible damage to electronics is the PVDIS configuration with 40cm Liquid Deuterium target, but the localisation of the leakage (close to the beam-line, see figures 44 ,45 and 46), and the low level of radiation present, suggest that a shielding construction is not needed. A further factor of 10 reduction, if needed, can probably be reached placing shielding material on the hot areas, around the beam-line, if this area, will be used during the experiment, reaching levels of radiation compatible also to commercial electronics.

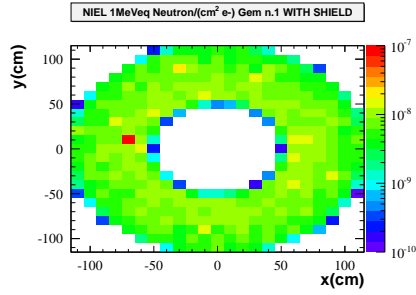
**Radiation with external targets** Some of the configuration with the SoLID spectrometer, position their target in the proximity of the entrance of the magnet. Simulations have been done in order to evaluate possible high radiation areas for electronics. An example for the possible areas of high radiation with these layouts for the experiments is shown in figure 47 (SIDIS configuration with  $^3\text{He}$  target).

## References

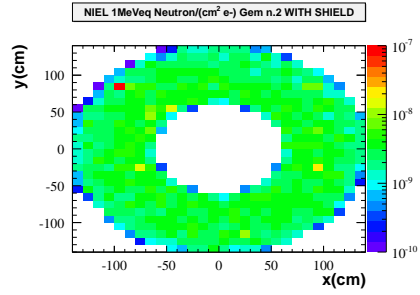
- [1] ROOT/C++ Analyzer for Hall A <http://hallaweb.jlab.org/podd/index.html>.
- [2] Fluka. <http://www.fluka.org>.
- [3] Geant4. <http://geant4.cern.ch/>.
- [4] Gemc. <https://gemc.jlab.org/>.
- [5] Poisson superfish. [http://laacg1.lanl.gov/laacg/services/download\\_sf.phtml](http://laacg1.lanl.gov/laacg/services/download_sf.phtml).
- [6] Tosca. <http://www.chilton-computing.org.uk/inf/eng/electromagnetics/p001.htm>.

- 2100 [7] Hall A. Hall a c++ analyzer. <http://hallaweb.jlab.org/podd/>.
- 2101 [8] C. Altunbas *et al.* *Nucl. Inst. Meth*, A490:177, 2002.
- 2102 [9] J.Huston H.L. Lai P. Nadolsky W.K. Tung J. Pumplin, D.R. Stump. *JHEP*,  
2103 0207:12, 2002.
- 2104 [10] G.M. Urciuli M. Capogni, E. Cisbani. Note on gem digitiation modeling.  
2105 <http://www.iss.infn.it/cisbani/atmp/gemc/code/>.
- 2106 [11] R. Mankel. *Rept. Prog. Phys*, 67:553, 2004.
- 2107 [12] D.E. Wiser. PhD thesis, University of Wisconsin-Madison, 1977.
- 2108 [13] *The FLUKA code: Description and benchmarking* G. Battistoni, S. Muraro,  
2109 P.R. Sala, F. Cerutti, A. Ferrari, S. Roesler, A. Fasso', J. Ranft, Proceedings  
2110 of the Hadronic Shower Simulation Workshop 2006, Fermilab 6–8 September  
2111 2006, M.Albrow, R. Raja eds., AIP Conference Proceeding 896, 31-49,  
2112 (2007)
- 2113 [14] *FLUKA: a multi-particle transport code* A. Ferrari, P.R. Sala, A. Fasso', and  
2114 J. Ranft, CERN-2005-10 (2005), INFN/TC\_05/11, SLAC-R-773
- 2115 [15] *Photodisintegration of deuterium and big bang nucleosynthesis* K.Y.Hare and  
2116 others, *Phys. Rev. D* 68, 072001 (2003)
- 2117 [16] *Displacement damage in silicon, on-line compilation* A. Vasilescu and G.  
2118 Lindstroem available at [http://hepweb03.phys.sinica.edu.tw/](http://hepweb03.phys.sinica.edu.tw/opto/Irradiation/Documents/NIEL_scaling/gunnar.htm)  
2119 [opto/Irradiation/Documents/NIEL\\_scaling/gunnar.htm](http://hepweb03.phys.sinica.edu.tw/opto/Irradiation/Documents/NIEL_scaling/gunnar.htm)

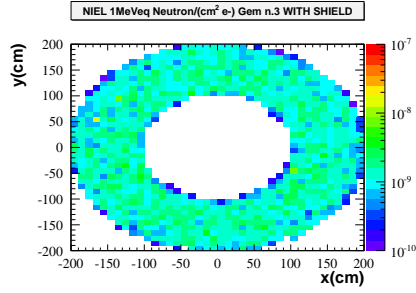




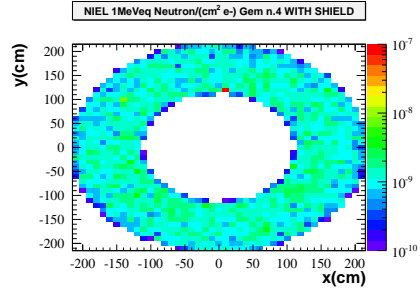
(a) NIEL weighted 1MeV equivalent neutron flux per  $cm^2$  per incident electron on the 1<sup>st</sup> GEM foil



(c) NIEL weighted 1MeV equivalent neutron flux per  $cm^2$  per incident electron on the 2<sup>nd</sup> GEM foil



(b) NIEL weighted 1MeV neutron equivalent neutron flux per  $cm^2$  per incident electron on the 3<sup>rd</sup> GEM foil



(d) NIEL weighted 1MeV equivalent neutron flux per  $cm^2$  per incident electron on the 4<sup>th</sup> GEM foil

Figure 39: The CMS experiment dose rates are expected to be of the order of 10 MRad( $SiO_2$ ) ( $5 \times 10^{13} \frac{n}{cm^2}$ ). This translate for us, assuming 2000 hours of beam at  $100\mu A$ , in a flux of  $\sim 1.1 \times 10^{-8} \frac{1MeVeqn}{e^-cm^2}$ . This put us on the same level of radiation that the APV25 chip was built to tolerate

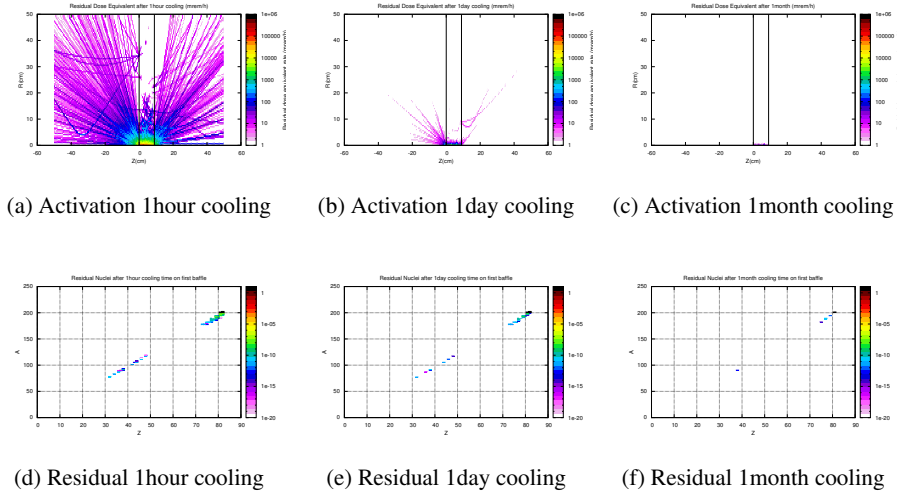


Figure 40: First Baffle: Activation study for 3 different Cooling times, after an assumed exposure to the beam of 3 separate full weeks intervalled by a down time of 4 days. (40a, 40b, 40c) The dose is expressed in  $mrem/h$  and here is shown their spatial distribution. (40d, 40e, 40f) The Residual decaying Nuclei are shown as a function of Z, A.

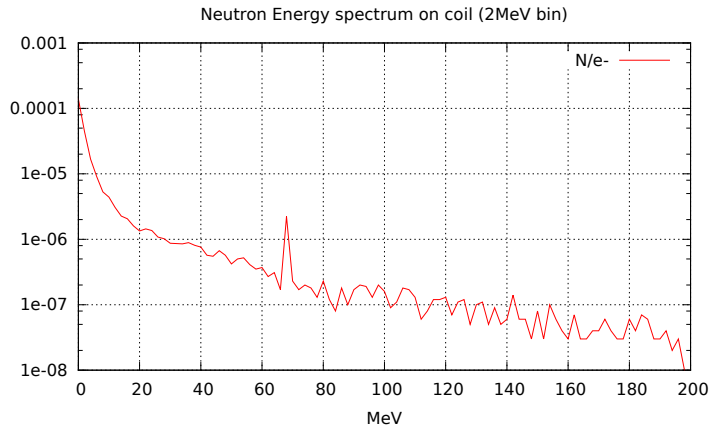
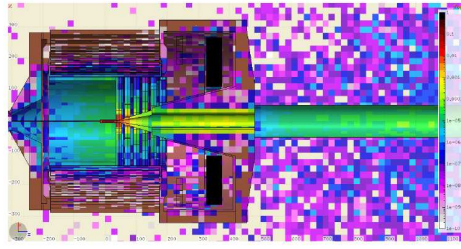
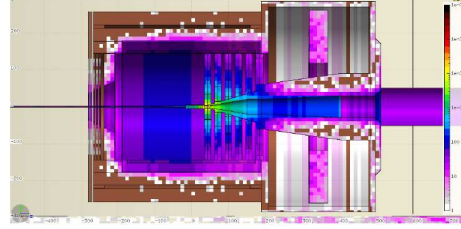


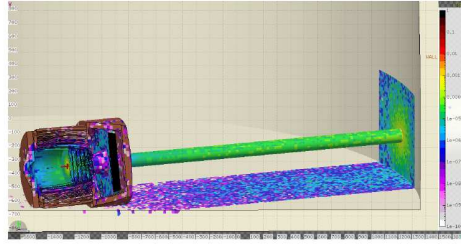
Figure 41: Neutron energy spectrum per electron on the magnet cryostat



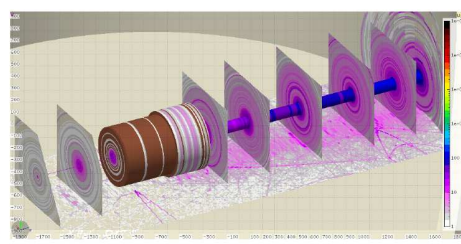
(a) Energy deposited (W) per  $cm^3$  for PVDIS configuration and Liquid Deuterium target



(c) Dose equivalent (mrem) per hour after 1 hour from beam exposure for PVDIS configuration and Liquid Deuterium target

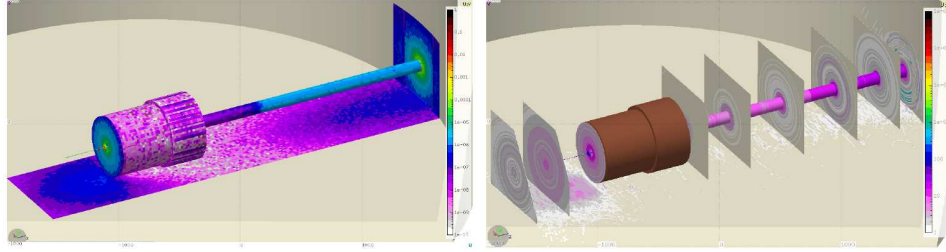


(b) Energy deposited (W) per  $cm^3$  for PVDIS configuration and Liquid Deuterium target (Hall view)

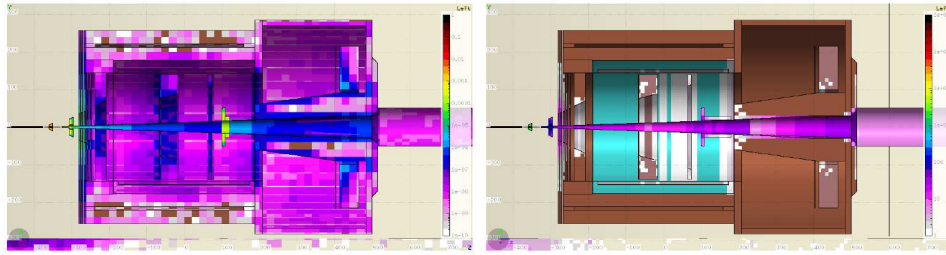


(d) Dose equivalent (mrem) per hour after 1 hour from beam exposure for PVDIS configuration and Liquid Deuterium target (Hall view)

Figure 42: Energy deposited (W) per  $cm^3$  (42a and 42b) considering running condition with Liquid Deuterium target and electron beam current of  $100\mu A$ . The spectrum is averaged in blocks of size of  $20cm \times 20cm \times 20cm$  in order to boost statistics, since this simulation with the complex SoLID design is very high demanding in CPU time. One can see how the power deposited in the first baffle region is considerably higher respect to the one expected in the exit hole of the magnet. In order to obtain the integrated power deposition for the expected beam time for the PVDIS configuration (2000h), multiply the values of the plots by  $7.2E+06$ . Activation dose equivalent (mrem) rate per hour (42c and 42d) expected with the same configuration after 1 hour from beam exposure (  $100\mu A$  for a month ). This study has been done in order to simulate condition in the Hall during running time. For a more accurate description of the activation expected in the baffle area, see figure 40



(a) Energy deposited (W) per  $cm^3$  considering (b) Dose equivalent (mrem) per hour after 1 hour  
SIDIS running condition with  $^3He$  target and elec-from beam exposure for SIDIS configuration and  
tron beam current of  $15\mu A$  (Hall view)  $^3He$  target (Hall view)



(c) Energy deposited (W) per  $cm^3$  considering (d) Dose equivalent (mrem) per hour after 1 hour  
SIDIS running condition with  $^3He$  target and elec-from beam exposure for SIDIS configuration and  
tron beam current of  $15\mu A$  (Inside the magnet)  $^3He$  target (Inside the magnet)

Figure 43: Energy deposited (W) per  $cm^3$  (43a 43c) considering running condition with  $^3He$  target and electron beam current of  $15\mu A$ . In order to obtain the integrated power deposition for the expected beam time for the SIDIS configuration (3000h), multiply the values of the plots by  $1.08E+07$ . The main part of the energy is deposited, as expected, in the target area and in the collimator positioned in front of the nosecone part of the magnet. The energy deposited in the exit hole of the magnet is considerably lower than with the PVDIS configuration. Activation dose equivalent (mrem) rate per hour (43b and 43d) expected with the same configuration after 1 hour from beam exposure (  $15\mu A$  for a month ). This study has been done in order to simulate condition in the Hall during running time.

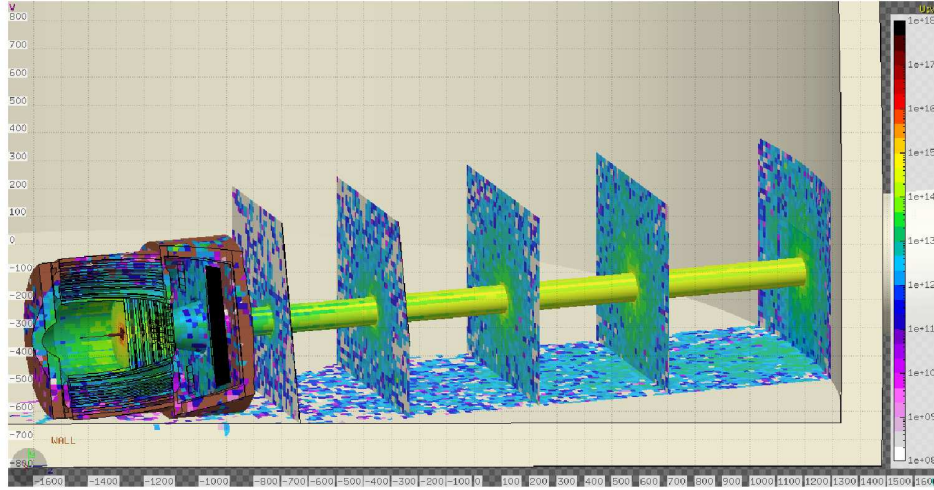


Figure 44: Estimate of radiation damage in the Hall with the SoLID spectrometer and the PVDIS configuration. The leading part of radiation present in the Hall for the SoLID spectrometer is leaking through the downstream part of the beam-line assembly. In this plot is shown the 1MeV Neutron equivalent flux per  $cm^2$  on the volumes surfaces estimated for 2000h of continuous running with a beam current of  $100\mu A$  (This is the expected beam-time with the PVDIS configuration). In order to better show the behaviour of the radiation leaking, different plane of observation have been inserted (at a distance from the target of  $\Delta z = 6m$ ,  $\Delta z = 10m$ ,  $\Delta z = 15m$ ,  $\Delta z = 20m$ ). The level of radiation leaking increases as one moves farther from the target, reaching a maximum  $\leq 10^{15} \frac{N_{1MeV}}{cm^2}$ . These levels of radiation is on the “mild to severe” damage range for commercial semiconductors ( as one can see comparing them with Estimate of the tolerance of different material plots 33). This area is not expected to carry any delicate equipment. On the upstream section of the beam-line, the level of radiation leaking is tolerable to also commercial equipment (not rad-hard). A comparable plot of this one, with a projection plane on the zy axis, is show in figure 45



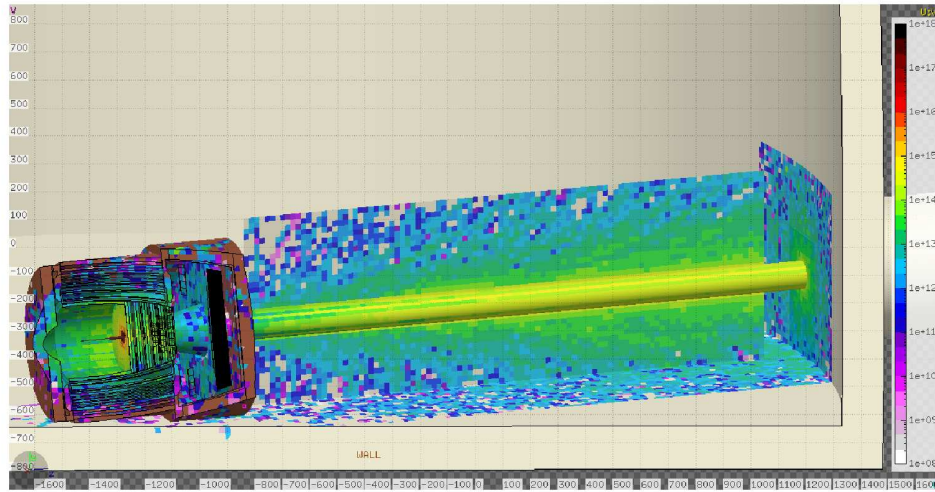


Figure 45: Estimate of radiation damage in the Hall with the SoLID spectrometer and the PVDIS configuration. A projection plane parallel to the beam-line is shown here to show full zy dependence of the 1MeV equivalent Neutron flux. For a full explanation see the caption of figure 44

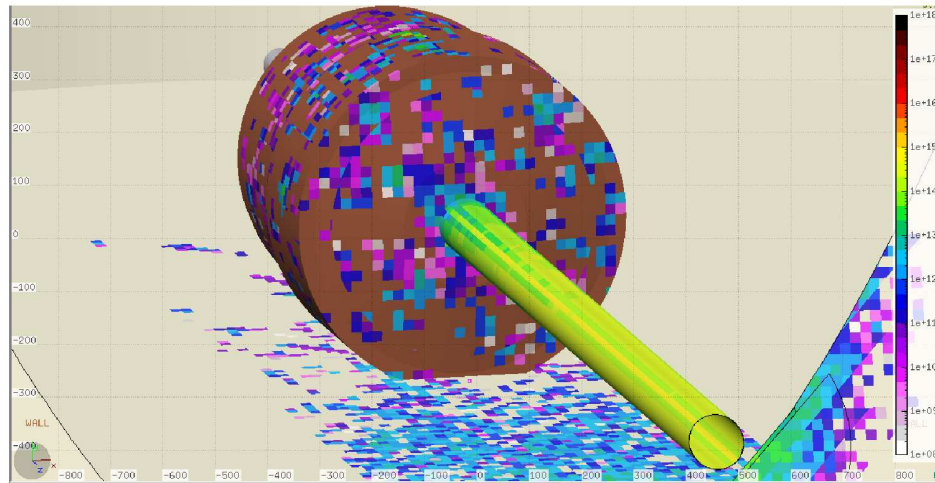


Figure 46: Estimate of radiation damage in the Hall with the SoLID spectrometer and the PVDIS configuration. View of the back part of the SoLID spectrometer. The predominant part of the leaking radiation is supposed to pass through the downstream beam-line.

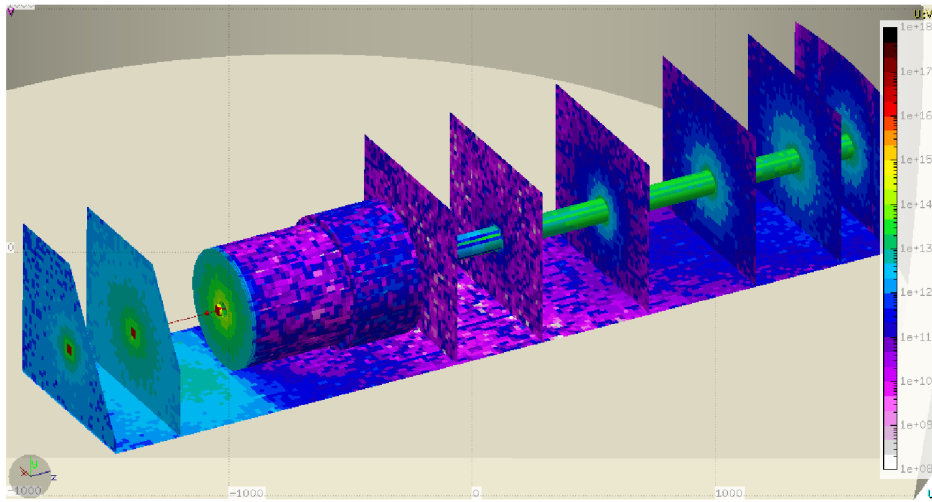


Figure 47: Estimate of radiation damage in the Hall with the SoLID spectrometer and the SIDIS  $^3\text{He}$  configuration. The leading part of radiation present in the Hall for the SoLID spectrometer is originating from the target area and the closer surface of the magnet. In this plot is shown the 1MeV Neutron equivalent flux per  $\text{cm}^2$  on the volumes surfaces estimated for 3000h of continuous running with a beam current of  $15\mu\text{A}$  (This is the expected beam-time with the SIDIS configuration). In order to better show the behaviour of the radiation leaking, different planes of observation have been inserted (at a distance from the centre of the Cryostat of the magnet of  $\Delta z = -10\text{m}$ ,  $\Delta z = -6\text{m}$ ,  $\Delta z = 6\text{m}$ ,  $\Delta z = 10\text{m}$ ,  $\Delta z = 15\text{m}$ ,  $\Delta z = 20\text{m}$ ,  $\Delta z = 24\text{m}$ ). The level of radiation leaking increases as one moves farther from the target, reaching a maximum  $< 10^{14} \frac{\text{N}_{1\text{MeV}}}{\text{cm}^2}$ . These levels of radiation is on the “mild to severe” damage range for commercial semiconductors ( as one can see comparing them with Estimate of the tolerance of different material plots 33). This area is not expected to carry any delicate equipment.